JOC*Article*

Photophysical and Electrochemical Properties of 1,7-Diaryl-Substituted Perylene Diimides

Chun-Chieh Chao[†] and Man-kit Leung*[,†,‡]

Department of Chemistry and Institute of Polymer Science and Engineering, National Taiwan University, Taipei, Taiwan 106, ROC

Yuhlong Oliver Su,* Kuo-Yuan Chiu, and Tsung-Hsien Lin

Department of Applied Chemistry, National Chi Nan University, Nantou, Taiwan 545, ROC

Shwu-Ju Shieh and Shien-Chang Lin

RiTdisplay Corporation, Hsin Chu Industrial Park, Taiwan 30351, ROC

mkleung@ntu.edu.tw

Received January 1, 2005

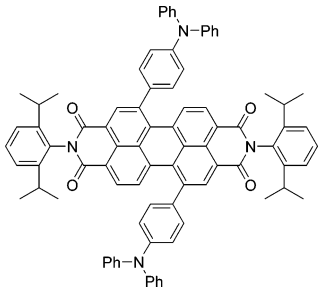

Substituent effects on the photophysical and electrochemical properties of 1,7-diaryl-substituted perylene diimides (1,7-Ar_2PDIs) have been carefully explored. Progressive red-shifts of the absorption and emission maxima were observed when the electron-donating ability of these substituents was increased. Linear Hammett correlations of $1/\lambda_{max}$ versus σ^+ were observed in both spectral analyses. The positive slopes of the Hammett plots suggested that the electronic transitions carry certain amounts of photoinduced intramolecular charge-transfer (PICT) character from the aryl substituents to the perylene diimide core which leads to the reduction of the electron density on the substituents. The substituent electronic effects originated mainly from the perturbation of the core PDI HOMO energy level by the substituents. This conclusion was supported by PM3 analyses and confirmed by cyclic voltammetry experiments. More interestingly, the $Ph_2NC_6H_4$-substituted PDI, **4i**, showed an unusual dual-band absorption that spans from 450 to 750 nm. We tentatively assigned these two bands as the charge-transfer band and the PDI core absorption, respectively.

Introduction

During the past few decades, conversion of solar energy into electricity has been one of the important areas for scientific research.[1] Today's silicon solar cells can convert up to 24% of the terrestrial solar energy into electrical energy and have been already commercialized for many applications.[2] However, the solar cell's production usually involves high-temperature processes as well as numerous lithographic steps.[3] Therefore, solar cells made from organic semiconducting thin films have become attractive alternatives to investigate. Organic semiconductors can conduct charges through partial delocalization or charge hopping between molecules.[4] Cells made from organic semiconductors have been of interest as photovoltaic light emitting devices, field effect transistors, and memories.[5] Current organic solar cells have reached solar power efficiencies of about 2% with corresponding external quantum efficiency peaks at about 50%.[6]

One important factor that governs the performance of a solar cell is the absorption spectrum of the organic semiconductors or the dye molecules used for device

[†] Department of Chemistry.
[‡] Institute of Polymer Science and Engineering.

10.1021/jo050001f CCC: $30.25
Published on Web 04/19/2005

SCHEME 1. Synthesis of 1,7-Ar$_2$PDIs

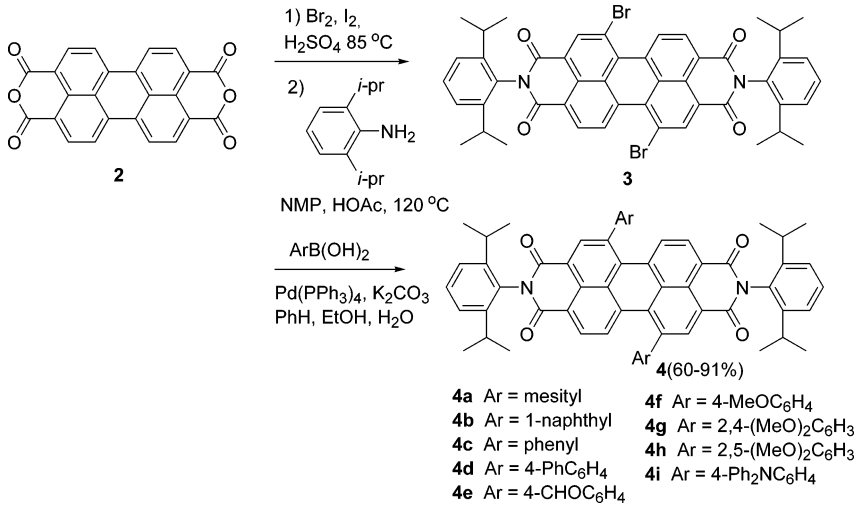

fabrication. In an ideal situation, the solar cell absorption spectrum should completely cover the region of terrestrial solar irradiation.[7] Therefore, the development of novel dye molecules with appropriate absorptive properties for photon harvesting has become an important area to explore. Organic dyes usually absorb photons through allowed $\pi-\pi^*$ or $n-\pi^*$ electronic transitions. Unfortunately, the absorption bands of organic chromophores are usually narrow and unable to cover the whole visible region. Therefore, multichromophoric materials have recently been developed.[8]

Perylene diimides (PDIs) are important electron acceptors and electron-transporting materials that have been used in various dimensions. In particular, PDIs show unusual photocurrent amplification properties and are potentially useful compounds for solar cell applications.[9] Therefore, it is extremely crucial to understand the photophysical properties of PDIs.

The parent PDI **1** shows a vibronic absorption band at 450−550 nm.[10]

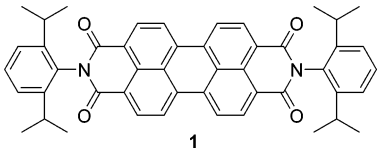

1

This absorption range is important because it is located in the middle of the visible region. However, the bandwidth is not wide enough to cover the spectral range. Introduction of conjugated substituents onto the perylene core is known to perturb the orbital energy of the perylene π-array and usually leads to a shift of the absorption maximum.[11] Nevertheless, the width of the absorption band would not be significantly expanded. Recently, imido *N*-substituent effects and multichromophoric perylene diimides with wide spectral responses have been investigated and reported.[12] In our report, we have described the synthesis and chromophoric behavior of 1,7-diaryl-substituted PDIs (1,7-Ar$_2$PDIs).

Results and Discussion

The synthesis of 1,7-Ar$_2$PDIs began with the I_2-catalyzed bromination of 3,4,9,10-perylenetetracarboxylic dianhydride (**2**) in 98% concentrated sulfuric acid (Scheme 1).[13] As mentioned in previous literature, high-field ^{1}H NMR analysis revealed that the crude product contained about 75% of the desired 1,7-isomers along with 25% of another unidentified isomer.[13a,14] Because of the low solubility of the crude product, purification of the dibromide is difficult. Therefore, the crude product was subjected to imidization without further purification. Imidization of the anhydride with 2,6-diisopropylaniline was carried out in acetic acid to smoothly produce diimide **3**. The unidentified isomer could be easily removed by recrystallization from toluene at this step. Suzuki coupling is known to be an effective approach for introducing aryl side groups to the perylene diimide core.[11a,15] Even though steric hindrance is expected to be high, Suzuki coupling of **3** with various boronic acids successfully produces **4** in high yields in our study.

Spectral Properties of 1,7-Ar$_2$PDIs. The synthetic yields of the 1,7-Ar$_2$PDIs prepared and their photophysi-

(1) (a) Coakley, K. M.; McGehee, M. D. *Chem. Mater.* **2004**, *16*, 4533−4542. (b) Veenstra, S. C.; Verhees, W. J. H.; Kroon, J. M.; Koetse, M. M.; Sweelssen, J.; Bastiaansen, J. J. A. M.; Schoo, H. F. M.; Yang, X.; Alexeev, A.; Loos, J.; Schubert, U. S.; Wienk, M. M. *Chem. Mater.* **2004**, *16*, 2503−2508. (c) Imahori, H.; Fukuzumi, S. *Adv. Funct. Mater.* **2004**, *14*, 525−536. (d) Kannan, B.; Castelino, K.; Majumdar, A. *Nano Lett.* **2003**, *3*, 1729−1733. (e) Sun, B.; Marx, E.; Greenham, N. C. *Nano Lett.* **2003**, *3*, 961−963. (f) Tokuhisa, H.; Hammond, P. T. *Adv. Funct. Mater.* **2003**, *13*, 831−839. (g) Wienk, M. M.; Kroon, J. M.; Verhees, W. J. H.; Knol, J.; Hummelen, J. C.; van Hal, P. A.; Janssen, R. A. J. *Angew. Chem., Int. Ed.* **2003**, *42*, 3371−3375. (h) van Hal, P. A.; Wienk, M. M.; Kroon, J. M.; Verhees, W. J. H.; Slooff, L. H.; van Gennip, W. J. H.; Jonkheijm, P.; Janssen, R. A. J. *Adv. Mater.* **2003**, *15*, 118−121. (i) Kim, Y.-G.; Walker, J.; Samuelson, L. A.; Kumar, J. *Nano Lett.* **2003**, *3*, 523−525. (j) Eckert, J.-F.; Nicoud, J.-F.; Nierengarten, J.-F.; Liu, S.-G.; Echegoyen, L.; Barigelletti, F.; Armaroli, N.; Ouali, L.; Krasnikov, V.; Hadziioannou, G. *J. Am. Chem. Soc.* **2000**, *122*, 7467−7479. (k) Zhang, F.; Johansson, M.; Andersson, M. R.; Hummelen, J. C.; Inganäs, O. *Adv. Mater.* **2002**, *14*, 662−665. (l) Snaith, H. J.; Arias, A. C.; Morteani, A. C.; Silva, C.; Friend, R. H. *Nano Lett.* **2002**, *2*, 1353−1357.

(2) (a) Green, M. A. *Adv. Mater.* **2001**, *13*, 1019−1022. (b) Schultz, O.; Glunz, S. W.; Willeke, G. P. *Prog. Photovoltaics* **2004**, *12*, 553−558. (c) Green, M. A.; Emery, K.; King, D. L.; Igari, S.; Warta, W. *Prog. Photovoltaics* **2004**, *12*, 365−372.

(3) (a) MacDiarmid, A. G. *Angew. Chem., Int. Ed.* **2001**, *40*, 2581−2590. (b) Ozin, G. A.; Yang, S. M. *Adv. Funct. Mater.* **2001**, *11*, 95−104 (c) Gonsalves, K. E.; Merhari, L.; Wu, H.; Hu, Y. *Adv. Mater.* **2001**, *13*, 703−714. (d) Zhong, Z.; Gates, B.; Xia, Y.; Qin, D. *Langmuir* **2000**, *16*, 10369−10375.

(4) (a) Sutin, N.; Brunschwig, B. S.; Creutz, C.; Feldberg, S. W. *J. Phys. Chem. B* **2004**, *108*, 12092−12102. (b) Heeney, M.; Bailey, C.; Giles, M.; Shkunov, M.; Sparrowe, D.; Tierney, S.; Zhang, W.; McCulloch, I. *Macromolecules* **2004**, *37*, 5250−5256. (c) Gregg, B. A. *J. Phys. Chem. B* **2003**, *107*, 4688−4698.

TABLE 1. Synthetic Yields and Photophysical Properties of Ar_2PDIs

compd	Ar	yield	λ_{max}(abs)	log ϵ^a	λ_{max}(fl)	Qy[b]
1	H	—[c]	527	4.90	534	1
3	Br	36	528	4.68	547	0.76
4a	mesityl	73	534	4.76	577	0.68
4b	1-naphthyl	80	540	4.60	625	0.30
4c	phenyl	90	556	4.62	594	0.61
4d	4-(Ph)C_6H_4	91	566	4.65	624	0.38
4e	4-(OCH)C_6H_4	70	550	4.63	587	0.55
4f	4-(MeO)C_6H_4	66	573	4.50	635	0.14
4g	2,4-$(MeO)_2C_6H_3$	70	563	4.50	640	0.08
4h	2,5-$(MeO)_2C_6H_3$	71	542	4.53	–	–
4i	4-$(Ph_2N)C_6H_4$	60	512, 653	4.57,4.13	–	–

[a] ϵ is the extinction coefficient in M^{-1} cm^{-1}. [b] Qy is the quantum yield. [c] Authentic sample.

cal properties are summarized in Table 1. All of these compounds are highly soluble in various organic solvents, such as CH_2Cl_2, $CHCl_3$, PhMe, and Me_2CO. The parent PDI shows an absorption band peak at 527 nm with characteristic vibronic fine structure (Figure 1) which is

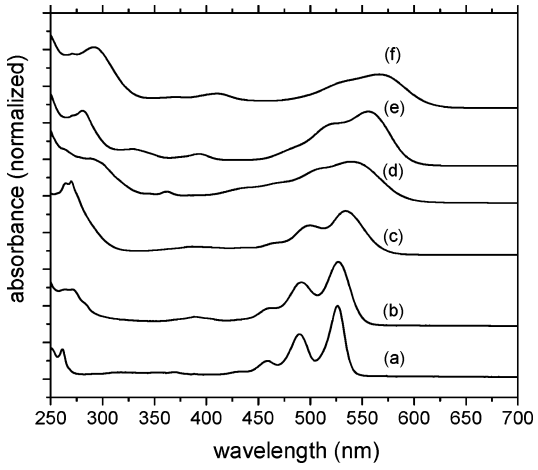

FIGURE 1. Normalized UV−vis absorption spectra for (a) **1** (λ_{max} = 527 nm), (b) **3** (λ_{max} = 528 nm), (c) **4a** (λ_{max} = 534 nm), (d) **4b** (λ_{max} = 540 nm), (e) **4c** (λ_{max} = 556 nm), and (f) **4d** (λ_{max} = 566 nm) in $CHCl_3$.

attributed to the perylene core $\pi-\pi^*$ transition. Similar absorptive features are observed for the Br- and mesityl-substituted PDIs, **3** and **4a**, respectively. Because of the steric restriction caused by the methyl substituents, the orientation of the mesityl ring is restricted orthogonally to the perylene ring, and hence, the π-conjugative interactions are minimal. As a consequence, the λ_{max} of **4a** is only shifted slightly by 7 nm to 534 nm.

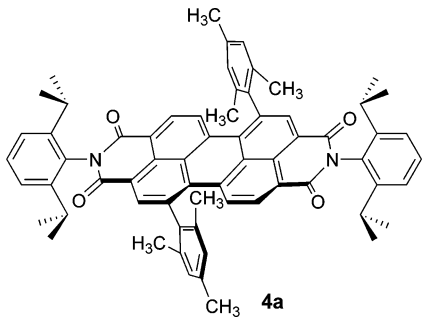

4a

For the 1-naphthyl-substituted PDI **4b**, two conformational diastereomers in a 1:1 ratio are observed from the

SCHEME 2. Schematic Diagrams for *anti*-4b and *syn*-4b

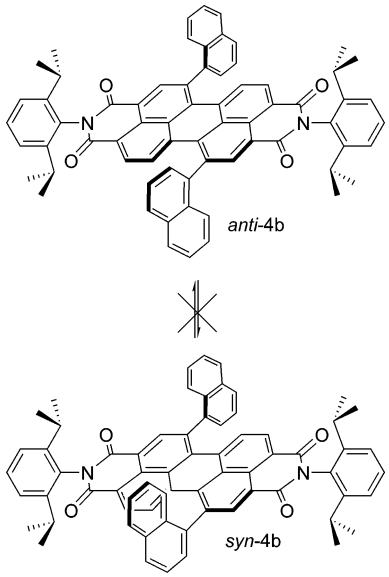

NMR analysis. We tentatively assigned them to the syn and anti forms. Perhaps because of a large restricted rotational energy barrier, the orientation of the naphthyl groups is also restricted perpendicularly to the perylene units. Interconversion between the syn and anti forms is hindered at room temperature, and thus, the red-shift effect in this case is also small (Scheme 2).

When the mesityl rings were replaced by phenyl groups, there were less steric restrictions on the dihedral

(5) (a) Li, A. D. Q.; Li, L. S. *J. Phys. Chem. B* **2004**, *108*, 12842−12850. (b) Haque, S. A.; Park, T.; Xu, C.; Koops, S.; Schulte, N.; Potter, R. J.; Holmes, A. B.; Durrant, J. R. *Adv. Funct. Mater.* **2004**, *14*, 435−440. (c) Anthopoulos, T. D.; Frampton, M. J.; Namdas, E. B.; Burn, P. L.; Samuel, I. D. W. *Adv. Mater.* **2004**, *16*, 557−560. (d) Kwon, T. W.; Alam, M. M.; Jenekhe, S. A. *Chem. Mater.* **2004**, *16*, 4657−4666. (e) Chen, X. L.; Lovinger, A. J.; Bao, Z.; Sapjeta, J. *Chem. Mater.* **2001**, *13*, 1341−1348. (f) Xiao, K.; Liu, Y.; Huang, X.; Xu, Y.; Yu, G.; Zhu, D. *J. Phys. Chem. B* **2003**, *107*, 9226−9230. (g) Ponomarenko, S. A.; Kirchmeyer, S.; Elschner, A.; Huisman, B.-H.; Karbach, A.; Drechsler, D. *Adv. Funct. Mater.* **2003**, *13*, 591−596. (h) Meng, H.; Zheng, J.; Lovinger, A. J.; Wang, B.-C.; Van Patten, P. G.; Bao, Z. *Chem. Mater.* **2003**, *15*, 1778−1787. (i) Ito, K.; Suzuki, T.; Sakamoto, Y.; Kubota, D.; Inoue, Y.; Sato, F.; Tokito, S. *Angew. Chem., Int. Ed.* **2003**, *42*, 1159−1162. (j) Veres, J.; Ogier, S. D.; Leeming, S. W.; Cupertino, D. C.; Khaffaf, S. M. *Adv. Funct. Mater.* **2003**, *13*, 199−204. (k) Katz, H. E.; Bao, Z.; Gilat, S. L. *Acc. Chem. Res.* **2001**, *34*, 359−369. (l) Videlot, C.; Ackermann, J.; Blanchard, P.; Raimundo, J.-M.; Frère, P.; Allain, M.; de Bettignies, R.; Levillain, E.; Roncali, J. *Adv. Mater.* **2003**, *15*, 306−310. (m) Mushrush, M.; Facchetti, A.; Lefenfeld, M.; Katz, H. E.; Marks, T. J. *J. Am. Chem. Soc.* **2003**, *125*, 9414−9423. (n) Kim, S. H.; Yang, Y. S.; Lee, J. H.; Lee, J.-I.; Chu, H. Y.; Lee, H.; Oh, J.; Do, L.-M.; Zyung, T. *Opt. Mater.* **2002**, *21*, 439−443.

angle. The phenyl groups of **4c** are allowed to rotate more freely leading to better π-orbital overlapping with the perylene core. This leads to a significant red-shift in the absorption spectrum in which the λ_{max} is shifted by 22 nm to 556 nm. Moreover, the vibronic pattern of the absorption spectrum becomes less clear. A further red-shift of the λ_{max} of biphenyl-substituted PDI **4d** to 566 nm implies that π-conjugation could be further extended in the biphenyl unit.

The spectral-broadening phenomena shown in Figure 1, from line (a) to line (f), could be attributed to two reasons. One could be the increase of the conjugation between the substituents and the perylene core.[11] Another could be the twisting of the perylene core by the substituents so that the vibronic structure is lost.[16] Previous X-ray crystallographic analyses[14,16] revealed that the PDI core should be twisted by the bay substituents at the 1,7-positions. If one compares the spectra of **1** (line a) against **4a** (line c), in which the π-conjugation is minimal, one can observe the twisting effect of the PDI core on spectral broadening. However, further spectral broadening along with significant red-shifting was observed in the comparison among the spectra of **4a** (line c), **4c** (line e), and **4d** (line f). Since the steric effects of the phenyl groups of **4a**, **4c**, and **4d** on the core twisting should not be significantly different, we tentatively attributed the spectral broadening to the π-conjugation effects. This argument is also consistent with the results of the semiempirical calculations that will be presented in later sections.

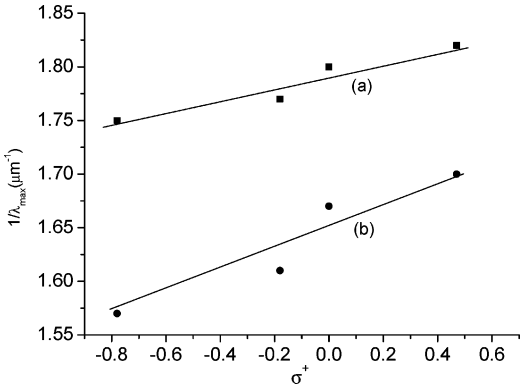

FIGURE 2. Hammett plot of $1/\lambda_{max}$ versus σ^+ for phenyl-substituted PDIs **4c**−**4f**: (a) absorption and (b) fluorescence.

Substituent electronic effects are also observed for 1,7-Ar_2PDIs. Progressive red-shifts of the absorption maxima occur when the electron-donating ability of the substituents increases. Since the perylene diimide core is known to be a good electron acceptor, photoinduced intramolecular charge transfer (PICT) may occur in this case. The photoinduced electronic transition would reallocate the electron density from the HOMO of the phenyl substituents to the LUMO of the perylene diimide core, re-siding the positive charge density on the phenyl substituents.[17] In this circumstance, the introduction of electron-donating groups on the phenyl substituents would stabilize the excited state, leading to significant red-shifts on their absorption spectra. This argument is supported by a reasonably good Hammett correlation of $1/\lambda_{max}$ versus σ^+ for the family of phenyl-substituted PDIs **4c**, **4d**, **4e**, and **4f** with a slope of $\rho_{abs} = +0.061\ \mu m^{-1}$ (Figure 2).[17] Compounds **4c**−**4f** were selected because they have similar steric factors and are, therefore, suitable models for comparison. The positive slope here suggested that the electronic transition carries a certain amount of PICT character from the phenyl substituent to the perylene diimide core which reduces the electron density on the phenyl substituent. On the the other hand, the spectral behavior of **4i** is quite different when compared to that of the others. The $1/\lambda_{max}$ of **4i** does not align well with the others in the Hammett plot. Furthermore, **4i** does not show any observable fluorescent properties. The photophysical properties of **4i** will therefore be discussed separately as another section.

Introduction of methoxy groups to the ortho positions again prohibits the phenyl ring from π-conjugation and, hence, reduces the red-shift effect on the λ_{max}. As we can see in the spectra shown in Figure 3, although **4g** and

(6) (a) Schmidt-Mende, L.; Fechtenkötter, A.; Müllen, K.; Moons, E.; Friend, R. H.; MacKenzie, J. D. *Science* **2001**, *293*, 1119−1122. (b) Vangeneugden, D. L.; Vanderzande, D. J. M.; Salbeck, J.; van Hal, P. A.; Janssen, R. A. J.; Hummelen, J. C.; Brabec, C. J.; Shaheen, S. E.; Sariciftci, N. S. *J. Phys. Chem. B* **2001**, *105*, 11106−11113.

(7) Hagfeldt, A.; Grätzel, M. *Acc. Chem. Res.* **2000**, *33*, 269−277.

(8) (a) Beckers, E. H. A.; Meskers, S. C. J.; Schenning, A. P. H. J.; Chen, Z.; Würthner, F.; Janssen, R. A. J. *J. Phys. Chem. A* **2004**, *108*, 6933−6937. (b) Law, K. Y. *Chem. Rev.* **1993**, *93*, 449−486.

(9) (a) Würthner, F.; Chen, Z.; Hoeben, F. J. M.; Osswald, P.; You, C.-C.; Jonkheijm, P.; Herrikhuyzen, J. v.; Schenning, A. P. H. J.; van der Schoot, P. P. A. M.; Meijer, E. W.; Beckers, E. H. A.; Meskers, S. C. J.; Janssen, R. A. J. *J. Am. Chem. Soc.* **2004**, *126*, 10611−10618. (b) Gregg, B. A. *J. Phys. Chem.* **1996**, *100*, 852−859. (c) Salaneck, W. R.; Seki, K.; Kahn, A.; Pireaux, J. J. *Conjugated Polymer and Molecular Interfaces*; Marcel Dekker: New York, 2001. (d) Neuteboom, E. E.; van Hal, P. A.; Janssen, R. A. J. *Chem.—Eur. J.* **2004**, *10*, 3907−3918. (e) Hua, J.; Meng, F.; Ding, F.; Li, F.; Tian, H. *J. Mater. Chem.* **2004**, *14*, 1849−1853. (f) You, C.-C.; Saha-Möller, C. R.; Würthner, F. *Chem. Commun*. **2004**, *18*, 2030−2031.

(10) (a) Geerts, Y.; Quante, H.; Platz, H.; Mahrt, R.; Hopmeier, M.; Böehm, A.; Müllen, K. *J. Mater. Chem.* **1998**, *8*, 2357−2369. (b) Holtrup, F.; Müller, G. R.; Quante, H.; De Feyter, S.; De Schryver, F. C.; Müllen, K. *Chem.—Eur. J.* **1997**, *3*, 219−225. (c) Seybold, G.; Wagenblast, G. *Dyes Pigm.* **1989**, *11*, 303−317.

(11) (a) Sugiyasu, K.; Fujita, N.; Shinkai, S. *Angew. Chem., Int. Ed.* **2004**, *43*, 1229−1233. (b) Kohl, C.; Weil, T.; Qu, J.; Müllen, K. *Chem.—Eur. J.* **2004**, *10*, 5297−5310.

(12) (a) Ahrens, M. J.; Sinks, L. E.; Rybtchinski, B.; Liu, W.; Jones, B. A.; Giaimo, J. M.; Gusev, A. V.; Goshe, A. J.; Tiede, D. M.; Wasielewski, M. R. *J. Am. Chem. Soc.* **2004**, *126*, 8284−8294. (b) Wang, Z. Y.; Qi, Y.; Gao, J. P.; Sacripante, G. G.; Sundararajan, P. R.; Duff, J. D. *Macromolecules* **1998**, *31*, 2075−2079. (c) Langhals, H.; Jona, W. *Angew. Chem., Int. Ed.* **1998**, *37*, 952−955. (d) Würthner, F.; Thalacker, C.; Sautter, A. *Adv. Mater*. **1999**, *11*, 754−758. (e) Langhals, H.; Saulich, S. *Chem.—Eur. J*. **2002**, *8*, 5630−5643. (f) Schweitzer, G.; Gronheid, R.; Jordens, S.; Lor, M.; De Belder, G.; Weil, T.; Reuther, E.; Müllen, K.; De Schryver, F. C. *J. Phys. Chem. A* **2003**, *107*, 3199−3207. (g) Langhals, H.; Ismael, R.; Yürük, O. *Tetrahedron* **2000**, *56*, 5435−5441. (h) Guo, X.; Zhang, D.; Zhang, H.; Fan, Q.; Xu, W.; Ai, X.; Fan, L.; Zhu, D. *Tetrahedron* **2003**, *59*, 4843−4850.

(13) (a) Rohr, U.; Kohl, C.; Müllen, K.; van de Craats, A.; Warman, J. *J. Mater. Chem.* **2001**, *11*, 1789−1799. (b) Böehm, A.; Arms, H.; Henning, G.; Blaschka, P. U.S. Patent 6184378, 2001. (c) Böehm, A.; Arms, H.; Henning, G.; Blaschka, P. U.S. Patent 6063181, 2000.

(14) Würthner, F.; Stepanenko, V.; Chen, Z.; Saha-Möller, C. R.; Kocher, N.; Stalke, D. *J. Org. Chem.* **2004**, *69*, 7933−7939.

(15) (a) Ahrens, M. J.; Fuller, M. J.; Wasielewski, M. R. *Chem. Mater.* **2003**, *15*, 2684−2686. (b) Serin, J. M.; Brousmiche, D. W.; Fréchet, J. M. J. *Chem. Commun.* **2002**, 2605−2607. (c) Rohr, U.; Schlichting, P.; Böhm, A.; Gross, M.; Meerholz, K.; Bräuchle, C.; Müllen, K. *Angew. Chem., Int. Ed.* **1998**, *37*, 1434−1437. (d) Miyaura, N.; Suzuki, A. *Chem. Rev.* **1995**, *95*, 2457−2483.

(16) (a) Osswald, P.; Leusser, D.; Stalke, D.; Würthner, F. *Angew. Chem., Int. Ed.* **2005**, *44*, 250−253. (b) Chen, Z.; Debije, M. G.; Debaerdemaeker, T.; Osswald, P.; Würthner, F. *ChemPhysChem* **2004**, *5*, 137−140.

(17) (a) Papper, V.; Pines, D.; Likhtenshtein, G.; Pines, E. *Photochem. Photobiol.* **1997**, *111*, 87−96. (b) Elango, K. P. *Trans. Met. Chem.* **2004**, *29*, 125−128. (c) Bonesi, S. M.; Fagnoni, M.; Albini, A. *J. Org. Chem.* **2004**, *69*, 928−935 and references therein.

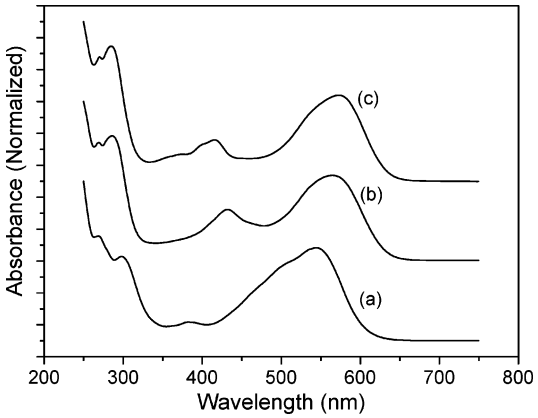

FIGURE 3. Normalized UV−vis absorption spectra for (a) **4h** (λ_{max} = 542 nm), (b) **4g** (λ_{max} = 563 nm), and (c) **4f** (λ_{max} = 573 nm) in $CHCl_3$.

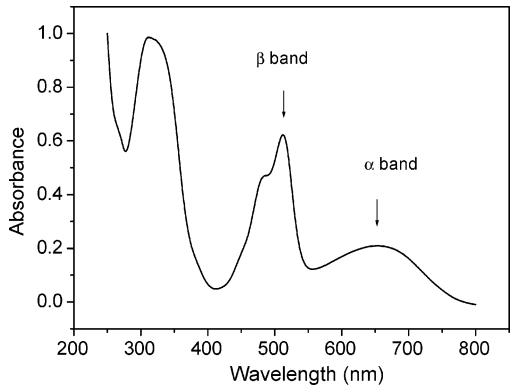

FIGURE 4. UV−vis absorption spectrum of **4i**.

4h are supposed to be more electron-rich than **4f**, **4f** has the largest red-shift on the λ_{max} in comparison with that of **4g** and **4h**.

More interesting is the fact that the absorption spectrum of 1,7-$(Ph_2NC_6H_4)_2$PDI (**4i**) shows dual bands in visible region, in which the first band, peaked at 653 nm, is denoted as the α-band and the second band, peaked at 512 nm, is denoted as the β-band (Figure 4). The first band is broad and is tentatively attributed to the charge-transfer absorption involving the electronic transition from the $C_6H_4NPh_2$ group to the electron-deficient perylene core. The second band shows a characteristic vibronic coupling pattern and is assigned to the perylene $\pi-\pi^*$ transition. The two absorption bands span a wide range of the visible spectrum from 450 to 750 nm. In comparison to the λ_{max} of the parent PDI, **1**, the α-band is shifted by 126 nm while the β-band is blue-shifted by 15 nm.

1,7-Ar_2PDIs **4a**−**4g** are fluorescent compounds. Their emissions, λ_{max}, are in the 577−640 nm range and are listed in Table 1. Their fluorescent spectra are shown in Figure 5. Similar substituent electronic effects have also been observed in their fluorescence spectra. A linear Hammett correlation of the $1/\lambda_{max}$ and the quantum yields of **4c**−**4f** and **4i** versus σ^+ are observed.[17] The larger slope of $\rho_{fl} = 0.107\ \mu m^{-1}$ (Figure 2) in comparison to $\rho_{abs} = 0.061\ \mu m^{-1}$ implies that the emissive excited state involved in the fluorescent process is more susceptible to the substituent electronic effects than that in the absorption process. This observation is consistent with the assumption that more positive charge will be re-sided onto the aryl substituents in the emissive excited state. In addition, the fluorescence quantum yield drops when the charge-transfer character increases (Figure 6). Therefore, perylene diimides containing electron-rich substituents such as **4f** and **4g** have low photo luminescence quantum yields, and the fluorescence of **4h** and **4i** are undetectable.

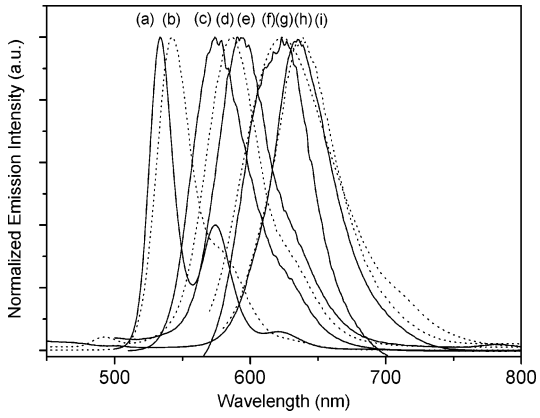

FIGURE 5. Normalized fluorescence spectra in $CHCl_3$ for (a) **1** (λ_{max} = 533 nm), (b) **3** (λ_{max} = 547 nm), (c) **4a** (λ_{max} = 577 nm), (d) **4e** (λ_{max} = 587 nm), (e) **4c** (λ_{max} = 594 nm), (f) **4d** (λ_{max} = 624 nm), (g) **4b** (λ_{max} = 625 nm), (h) **4f** (λ_{max} = 635 nm), and (i) **4g** (λ_{max} = 640 nm).

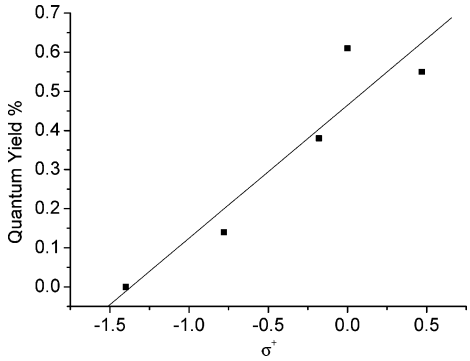

FIGURE 6. Hammett plot of fluorescence quantum yields versus σ for phenyl-substituted PDIs **4c**−**4f** and **4i**. The correlation coefficient is 0.94. The quantum yield is assumed to be zero in the plot.

To obtain insights into the origin of the spectral behavior, we analyzed the PDIs by semiempirical quantum computations in two ways: (1) optimizing the PDI structures by MM2 methods followed by PM3-RHF calculations for the HOMO and LUMO energies and (2) calculating individually the energy levels of the HOMOs and LUMOs of the perylene diimide core and the side groups by the semiempirical PM3-RHF computations for orbital analysis. To simplify the calculations, we used *N*-methyl groups to replace the large *N*-(2,6-diisopropylphenyl) groups in the calculations.

MM2-PM3 Calculations. The geometry optimizations were carried out by the MM2 method. The energies of the HOMO and LUMO of the corresponding structures were calculated by the PM3 method. The data are summarized in Table 2. As predicted from the literature,[14b,16] the structurally optimized PDI cores are twisted by an angle of 22−25°. The substituents have strong

TABLE 2. MM2-PM3/RHF Calculation of the HOMO−LUMO Energies of 4c−4f and 4i

compd	twisting angle (deg)[a]	HOMO (eV)	LUMO (eV)
4c	22.3	−8.717	−2.405
4d	25.5	−8.637	−2.424
4e	23.0	−8.919	−2.625
4f	23.8	−8.615	−2.388
4i	23.3	−8.077	−2.354

[a] The average angle from both sides of the optimized structure is not completely symmetrical.

TABLE 3. PM3/RHF Orbital Energies of Molecular Fragments

	HOMO (eV)	LUMO (eV)
PDI	−8.90	−2.48
Ph_3N	−7.94	0.04
$MeOC_6H_5$	−9.11	0.35
$(C_6H_5)_2$	−9.12	−0.17
C_6H_6	−9.75	0.40
$CHOC_6H_5$	−10.15	−0.75

perturbations on the HOMO energies. The variation of the HOMO energies of **4c**−**4f** is 0.304 eV. Unexpected strong perturbation on the HOMO from the electron-donating $Ph_2NC_6H_4$ substituents is observed in the calculation. The HOMO energy of **4i** is −8.077 eV which is much higher than that of the others. Pictorial orbital analysis revealed that the HOMOs of **4c**−**4f** originate from the PDI core. However, the HOMO of **4i** originates from the $Ph_2NC_6H_4$ group. On the other hand, the variation of the LUMO energies of **4c**, **4d**, **4f**, and **4i** is only 0.07 eV, a relatively smaller number than that of the HOMO energies. The LUMO energy of the most electron-deficient compound in the series, **4e**, is 2.625 eV, which is 0.313 eV lower than that of **4c**. Orbital analysis revealed that the LUMO originates from the PDI core, no matter whether the substituents are electron-deficient or electron-rich.

Orbital Analysis. To analyze the orbital interactions between the core and the aryl substituent, we determined the HOMO and LUMO energy levels of the substituent as well as the PDI core. Here, we assumed that the relative orbital energies could be reasonably approximated by the orbital energies of the corresponding molecular fragments. The data of the corresponding molecular fragments are listed in Table 3. The values for the HOMO and LUMO of the perylene diimide core are obtained on the basis of the assumption that the twisting angle is 22.3°.

As shown in Table 2, the orbital energies of the HOMOs of the $MeOC_6H_5$, PhC_6H_4, and Ph groups were estimated to be 0.3−0.8 eV lower than that of the perylene core. In these cases, the HOMO−HOMO interactions would raise the energy level of the core PDI HOMO and lower the energy level of the substituent HOMO (Scheme 3, right). On the other hand, the LUMOs of the side groups are 2.3−2.9 eV above the core PDI LUMO so that their interactions would be relatively small. Therefore, we concluded that substituent perturbation raises the HOMO of the PDI core and leads to a red-shift of the absorption spectrum. Since the HOMO of 1,7-Ar_2PDI involves orbital mixing of the substituents and the PDI unit while the LUMO mainly originates from the PDI core, photoexcitation of the HOMO electron onto

SCHEME 3

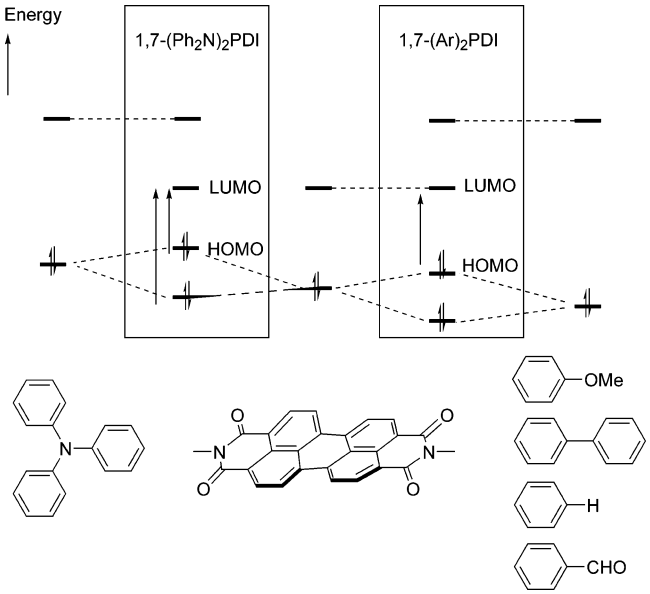

TABLE 4. Oxidation and Reduction $E_{1/2}$ Potentials[a] for 1,7-Ar_2PDIs

	oxidation[b]		reduction		
PDIs	2nd	1st	1st	2nd	3rd[b]
4-(OCH)C_6H_4		+1.83	−0.32	−0.54	−1.88
Br			−0.36	−0.56	−2.0
2,4,6-$(Me)_3C_6H_2$			−0.39	−0.64	
4-(MeO)C_6H_4		+1.54	−0.42	−0.65	
4-$(Ph_2N)C_6H_4$		+1.13	−0.44	−0.64	
C_6H_5		+1.70	−0.44	−0.64	
4-(Ph)C_6H_4		+1.65	−0.48	−0.74	
1-naphthyl		+1.75	−0.50	−0.77	
2,5-$(MeO)_2C_6H_3$	+1.60	+1.43	−0.54	−0.79	
2,4-$(MeO)_2C_6H_3$		+1.53	−0.57	−0.82	

[a] Versus Ag/AgCl electrode. [b] Irreversible wave.

the PDI LUMO would lead to some charge-transfer character from the aryl side groups to the PDI core.

On the other hand, the HOMO of the $Ph_2NC_6H_4$ group was found to be 1 eV above the core HOMO. Orbital interactions would lower the energy level of the PDI HOMO and raise the energy level of the $Ph_2NC_6H_4$ group's HOMO. Therefore, the HOMO of **4i** mainly originates from the HOMO of the $Ph_2NC_6H_4$ units. The absorption band at 653 nm is assigned to the charge-transfer absorption, involving the electronic transition from the HOMO of the $Ph_2NC_4H_4$ group to the LUMO of PDI. On the other hand, the blue-shifted absorption maximum at 512 nm was assigned to the electronic transition from the PDI HOMO to the PDI LUMO.

To further confirm our theoretical conclusions, we employed cyclic voltammetry to evaluate the substituent effects on the HOMO and LUMO of the perylene core. The experiments were carried out in CH_3CN or in a mixed solvent of CH_3CN and CH_2Cl_2 (1:1) in the presence of Bu_4NClO_4 as the supporting electrolyte. Their redox $E_{1/2}$ values and reversibility are summarized in Table 4.

To avoid interference from steric factors, we again selected a series of para-substituted derivatives, including the 4-CHO-, 4-H-, 4-Ph-, 4-MeO-, and 4-Ph_2N-substituted Ph_2PDIs **4c**, **4d**, **4e**, **4f**, and **4i**, respectively,

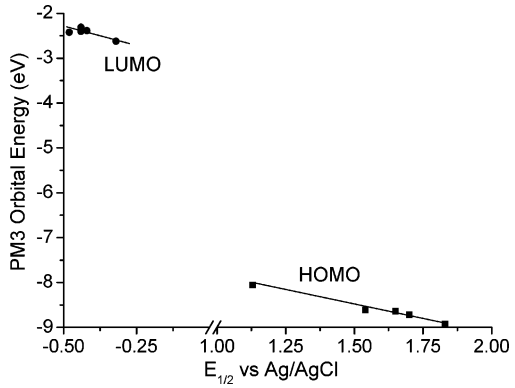

FIGURE 7. Correlation plots of the PM3 HOMO and LUMO energies versus the oxidation and the first reduction $E_{1/2}$ values from the CV experiments.

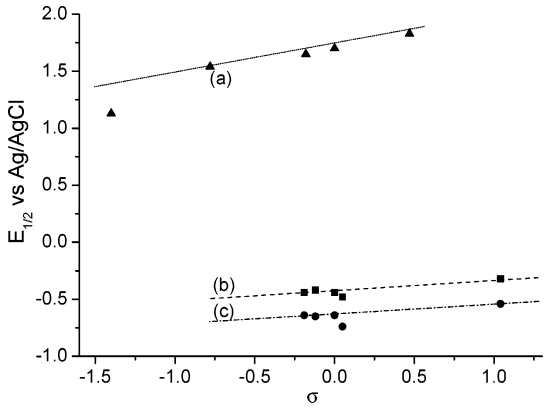

FIGURE 8. Hammett plot of $E_{1/2}$ (vs Ag/AgCl) versus σ for phenyl-substituted PDIs **4c**−**4f** and **4i**: (a) the first oxidation wave, (b) the first reduction wave, and (c) the second reduction wave. The σ^+ values were used for Ph_2N, MeO, and Ph groups in the oxidation plot. The σ^- value was used for CHO in the reduction plots.

for comparison. Most of the PDIs show one oxidation wave and two reduction waves, similar to the results reported in the literature.[18] Figure 7 shows the correlation plots of the orbital energies versus the $E_{1/2}$ values of the redox waves in the CV experiments. Reasonably good linear correlations in both plots support the validity of the above theoretical analysis.

Figure 8 shows the Hammett plots of the $E_{1/2}$ (vs Ag/AgCl) versus σ for phenyl-substituted PDIs **4c**−**4f** and **4i**. Substituent electronic effects are clearly observed on the oxidation waves of substituted PDIs. A progressive shift of the first oxidation potential to a low value was observed when the electron-donating ability of the substituents was increased. The difference between the oxidative $E_{1/2}$ values of **4e** and **4f** is 0.29 V. A good Hammett correlation of $1/\lambda_{max}$ versus σ^+ was observed for the first four derivatives with a slope of $\rho_{abs} = 230$ mV. The correlation coefficient is 0.99. The linearity of the plot against σ^+ with the positive slope suggested that the partial positive charge would be delocalized onto the phenyl side chains. On the other hand, the $E_{1/2}$ of **4i** is unusually low and away from the regression line. This observation is in good agreement with our theoretical prediction as well as the absorptive spectral data. It is noteworthy to remember that the $C_6H_4NPh_2$ units contain a high-lying HOMO. Therefore, the $C_6H_4NPh_2$ unit should have major contribution to the HOMO of **4i**. Electrochemical oxidation would, therefore, occur on the $C_6H_4NPh_2$ units at particularly low oxidation potentials that do not follow the trend of the Hammett plot.

Although one may consider the dimethoxy-substituted phenyl groups as electron-rich substituents, the introduction of methoxy groups at the ortho position sterically restricts the phenyl ring orthogonally to the perylene core and hence partially offsets the electron-donating power of the methoxy substituents. Therefore, the difference of redox potentials of 4-(MeO)C_6H_4-, 2,5-$(MeO)_2C_6H_2$-, and 2,4-$(MeO)_2C_6H_2$-substituted PDIs **4f**−**4h** is small.

On the the other hand, the variation of the reductive half potentials of C_6H_5-, 4-(Ph)C_6H_4-, 4-(MeO)C_6H_4-, and 4-$(Ph_2N)C_6H_4$-substituted PDIs is 0.06 V, a relatively small value. Even the difference of the reductive $E_{1/2}$ between **4e** and **4f** is only around 0.1 V. The slope of the Hammett plot was found to be 104 mV with a correlation coefficient of 0.87. A similar situation occurs on the second reduction wave, indicating that the substituent effects on the reduction potentials are small. The slope of the Hammett plot was found to be 100 mV with a correlation coefficient of 0.71. These results are in good agreement with our theoretical prediction in which the perturbation effects on the LUMO by substituents are less.

In summary, we reported the salient substituent effects on the photophysical and electrochemical properties of the PDI core. PDI molecule **4i** has unusual dual-band absorption that spans from 450 to 750 nm. Application of these molecules for solar cells and optoelectronics is under investigation.

Experimental Section

Materials. Compound **2**, $Pd(PPh_3)_4$, and Na_2CO_3 were purchased from a commercial supplier. All other reagents and solvents were of analytical or chemical grade and were purified using standard methods.

Procedure for the UV−Vis Absorption and Fluorescence Measurements. UV−vis and fluorescence spectra were collected between 200 and 900 nm for the compounds in $CHCl_3$. The quantum yields were measured by comparison against **1** as the standard. Compound **1** is known to have a quantum yield of 1.[10c]

Procedures for Cyclic Voltammetric (CV) Measurements. Electrochemical oxidation and reduction behavior of **4a**−**4i** were measured by CV (0−1.5 V, 100 mV/s) in CH_3CN or CH_3CN/CH_2Cl_2 (1:1) using Bu_4NClO_4 (0.1 M) or Bu_4NPF_6 (0.1 M) as the supporting electrolyte. The signals were obtained on a glassy-carbon working electrode with a Pt wire as the counter electrode and a Ag/AgCl (saturated) electrode as the reference electrode.

Methods for Theoretical Calculations. Semiempirical calculations were carried out by employing MM2 (Chem 3D) for structural optimization and PM3 (Cauche Company) for orbital analysis.

***N,N'*-Bis(2,6-diisopropylphenyl)-1,7-dibromoperylene-3,4,9,10-tetracarboxydiimide (3).**[19] Perylene-3,4,9,10-tetracarboxylic dianhydride **2** (32.0 g, 81.4 mmol), iodine (0.77 g, 3.03 mmol), and sulfuric acid (98%, 450 mL) were premixed and stirred for 2 h at room temperature. The reaction tem-

(18) (a) Lee, S. K.; Zu, Y.; Herrmann, A.; Geerts, Y.; Müllen, K.; Bard, A. J. *J. Am. Chem. Soc.* **1999**, *121*, 3513−3520. (b) Lu, W.; Gao, J. P.; Wang, Z. Y.; Qi, Y.; Sacripante, G. G.; Duff, J. D.; Sundararajan, P. R. *Macromolecules* **1999**, *32*, 8880−8885.

perature was set at 80 °C, and bromine (9.2 mL, 180 mmol) was added dropwise over 2 h. The mixture was reacted further at 80 °C for 16 h. The reaction mixture was cooled to room temperature, and the excess Br_2 was displaced by nitrogen. The product was precipitated by addition of ice−water and collected by suction filtration. The precipitate was washed with water several times until the aqueous layer became neutral to yield dibromo dianhydride as a crude product. The crude product was then dried under reduced pressure at 120 °C and used for the next step without further purification.

The crude 1,7-dibromoperylene-3,4,9,10-tetracarboxylic dianhydride (80 g, 14.5 mmol), excess 2,6-diisopropylaniline (88 mL, 46.7 mmol), and acetic acid (46 mL) were mixed and heated at 120 °C in NMP (1 L) under a nitrogen atmosphere for 120 h. The product was precipitated by the addition of water and collected by suction filtration. The crude product was washed with water until neutral and dried. The crude product was first purified by column chromatography on silica gel using CH_2Cl_2 as the eluent to obtain a mixture of the isomeric diimides. The mixture was washed with EtOH (300 mL) and toluene (300 mL) and then heated at 80 °C in toluene (300 mL) for 12 h. The pure diimide was recrystallized from the hot toluene solution. The crystals were collected through hot filtration to provide an essentially pure orange compound, **3** (46 g, 36% overall yield): ^{1}H NMR (400 MHz, $CDCl_3$) δ 9.56 (d, J = 8.0 Hz, 2H), 9.01 (s, 2 H), 8.79 (d, J = 8.0 Hz, 2H), 7.50 (t, J = 8.0 Hz, 2H), 7.35 (d, J = 8.0 Hz, 4H), 2.73 (septet, J = 6.8 Hz, 4H), 1.18 (d, J = 6.8 Hz, 24H); ^{13}C NMR (100 MHz, $CDCl_3$) δ 162.8, 162.3, 145.4, 138.3, 133.3, 133.1, 130.5, 129.96, 129.75, 129.48, 128.8, 127.5, 124.1, 123.1, 122.7, 120.9, 29.4, 24.1, 24.1; HRFAB *m/z* 869.1422, calcd for $C_{48}H_{40}Br_2N_2O_4$ *m/z* 866.1355.

A General Procedure for the Preparation of 1,7-Ar$_2$PDI. *N,N′*-Bis(2,6-diisopropylphenyl)-1,7-bis(2,4,6-trimethylphenyl)perylene-3,4,9,10-tetracarboxydiimide (4a). A deaerated mixture of EtOH (8.2 mL), benzene (47 mL), and H_2O (23 mL) was added to a solid mixture of **3** (7.0 g, 8.1 mmol), 2,4,6-trimethylphenylboronic acid[20] (10.6 g, 64.6 mmol), $Pd(PPh_3)_4$ (466 mg, 5.0 mol %), and Na_2CO_3 (2.56 g, 24.2 mmol) under nitrogen. The mixture was reacted at 80 °C for 120 h. The reaction was quenched by the addition of water. The mixture was extracted with CH_2Cl_2 several times. The combined organic layer was dried over anhydrous $MgSO_4$ and concentrated under reduced pressure to provide a crude solid. The crude solid was further purified by column chromatography on silica gel using toluene/CH_2Cl_2 (1:1) as the eluent to obtain **4a** as an orange red solid (5.5 g, 72%): mp > 380 °C dec; ^{1}H NMR (400 MHz, $CDCl_3$) δ 8.44 (s, 2H), 8.30 (d, J = 8.0 Hz, 2H), 8.12 (d, J = 8.0 Hz, 2H), 7.47 (t, J = 7.6 Hz, 2H), 7.32 (d, J = 7.6 Hz, 4H), 7.09 (s, 4H), 2.74 (septet, J = 6.4 Hz, 4H), 2.42 (s, 6H), 2.03 (s, 12H), 1.15 (d, J = 6.4 Hz, 24H); ^{13}C NMR (100 MHz, $CDCl_3$) δ 163.4, 163.1, 145.5, 139.6, 138.8, 138.23, 136.1, 135.9, 134.0, 133.2, 130.9, 130.3, 130.0, 129.6, 128.5, 128.5, 127.0, 124.0, 122.6, 122.2, 29.3, 24.2, 21.4, 20.9; HRFAB *m/z* 947.4796, calcd for $C_{66}H_{62}N_2O_4$ *m/z* 946.4710. Anal. Calcd for $C_{66}H_{62}N_2O_4$: C, 83.69; H, 6.60; N, 2.96. Found: C, 83.79; H, 6.42; N, 2.89.

***syn*- and *anti*-*N,N′*-Bis(2,6-diisopropylphenyl)-1,7-dinaphth-1-ylperylene-3,4,9,10-tetracarboxydiimide (4b).** The reaction of **3** (3.0 g, 3.5 mmol), 1-naphthaleneboronic acid[21] (4.76 g, 27.7 mmol), $Pd(PPh_3)_4$ (100 mg, 2.5 mol %), and Na_2CO_3 (1.10 g, 10.4 mmol) in degassed EtOH (3.5 mL), benzene (20 mL), and H_2O (10 mL) under nitrogen at 80 °C for 12 h followed by column chromatography purification on silica gel using toluene/CH_2Cl_2 (1:1) as the eluent produced **4b** (two conformational isomers, 1:1 ratio) as a red solid (2.7 g, 84%): mp > 390 °C dec; ^{1}H NMR (400 MHz, $CDCl_3$) δ 8.69, 8.67 (two conformers (1:1), s, 2H), 8.06−8.00 (m, 6H), 7.93−7.90 (m, 2H), 7.85 (d, J = 8 Hz, 1H), 7.79 (d, J = 8.0 Hz, 1H), 7.69−7.39 (m, 10H), 7.28 (d, J = 7.6 Hz, 4H), 2.73−2.66 (m, 4H), 1.15−1.07 (m, 24H); ^{13}C NMR (100 MHz, $CDCl_3$) δ 163.2, 163.1, 145.5, 145.4, 140.1, 140.0, 139.4, 139.2, 136.7, 136.6, 135.3, 135.2, 134.4, 134.3, 134.1, 134.0, 130.7, 130.5, 130.4, 130.3, 130.2, 129.5, 129.4, 129.2, 129.04, 128.97, 128.9, 128.6, 128.5, 127.5, 127.3, 127.1, 126.8, 126.72, 126.67, 126.44, 126.37, 124.7, 124.6, 123.9, 122.2, 122.0, 29.24, 29.22, 24.15, 24.10; HRFAB *m/z* 963.4158, calcd for $C_{68}H_{54}N_2O_4$ *m/z* 962.4084. Anal. Calcd for $C_{68}H_{54}N_2O_4$: C, 84.80; H, 5.65; N, 2.91. Found: C, 85.05; H, 5.75; N, 2.76.

***N,N′*-Bis(2,6-diisopropylphenyl)-1,7-diphenylperylene-3,4,9,10-tetracarboxydiimide (4c).** The reaction of **3** (3.0 g, 3.5 mmol), phenylboronic acid[22] (3.38 g, 27.7 mmol), $Pd(PPh_3)_4$ (100 mg, 2.5 mol %), and Na_2CO_3 (1.10 g, 10.4 mmol) in degassed EtOH (3.5 mL), benzene (20 mL), and H_2O (10 mL) at 80 °C for 8 h followed by column chromatographic purification on silica gel using toluene/CH_2Cl_2 (1:1) as the eluent produced **4c** as a red solid (2.7 g, 90%): mp > 390 °C dec; ^{1}H NMR (400 MHz, $CDCl_3$) δ 8.71 (s, 2H), 8.20 (d, J = 8.0 Hz, 2H), 7.92 (d, J = 8.0 Hz, 2H), 7.62 (dd, J = 8.0, 1.6 Hz, 4H), 7.53−7.45 (m, 8H), 7.32 (d, J = 8.0 Hz, 4H), 2.74 (septet, J = 6.8 Hz, 4H), 1.15 (m, 24H); ^{13}C NMR (100 MHz, $CDCl_3$) δ 163.27, 163.24, 145.4, 141.9, 141.27, 135.7, 135.2, 132.9, 130.4, 130.3, 130.2, 129.9, 129.5, 129.5, 128.9, 128.7, 128.3, 124.0, 122.2, 121.8, 29.3, 24.2, 24.1; HRFAB *m/z* 863.3862, calcd for *m/z* $C_{60}H_{50}N_2O_4$ 862.3771. Anal. Calcd for $C_{60}H_{50}N_2O_4$: C, 83.50; H, 5.84; N, 3.25. Found: C, 83.54; H, 5.63; N, 3.17.

***N,N′*-Bis(2,6-diisopropylphenyl)-1,7-bis(biphenyl-4-yl)-perylene-3,4,9,10-tetracarboxydiimide (4d).** The reaction of **3** (3.0 g, 3.5 mmol), biphenyl-4-boronic acid[23] (5.48 g, 27.7 mmol), $Pd(PPh_3)_4$ (100 mg, 2.5 mol %), and Na_2CO_3 (1.10 g, 10.4 mmol) in degassed EtOH (3.5 mL), benzene (20 mL), and H_2O (10 mL) under nitrogen at 80 °C for 12 h followed by column chromatographic purification on silica gel using toluene/CH_2Cl_2 (1:1) as the eluent produced **4d** as a red solid (91%, 3.2 g): mp > 390 °C dec; ^{1}H NMR (400 MHz, $CDCl_3$) δ 8.76 (s, 2H), 8.24 (d, J = 8.0 Hz, 2H), 8.09 (d, J = 8.0 Hz, 2H), 7.79−7.70 (m, 12H), 7.51−7.45 (m, 6H), 7.40 (t, J = 8.0 Hz, 2H), 7.33 (d, J = 8.0 Hz, 4H), 2.76 (septet, J = 6.8 Hz, 4H), 1.81−1.15 (m, 24H); ^{13}C NMR (100 MHz, $CDCl_3$) δ 163.3, 163.2, 145.4, 141.5, 140.9, 140.8, 139.8, 135.8, 135.3, 132.9, 130.4, 130.3, 123.0, 129.6, 129.54, 129.47, 128.9, 128.8, 128.3, 127.8, 127.0, 124.0, 122.3, 121.9, 29.3, 24.2, 24.1; HRFAB *m/z* 1015.4472, calcd for $C_{72}H_{58}N_2O_4$ *m/z* 1014.4397. Anal. Calcd for $C_{60}H_{50}N_2O_4$: C, 85.18; H, 5.78; N, 2.76. Found: C, 85.04; H, 5.78; N, 2.89.

***N,N′*-Bis(2,6-diisopropylphenyl)-1,7-di(4-formylphenyl)-perylene-3,4,9,10-tetracarboxydiimide (4e).** The reaction of **3** (3.0 g, 3.5 mmol), 4-formylphenylboronic acid[24] (4.15 g, 27.7 mmol), $Pd(PPh_3)_4$ (100 mg, 2.5 mol %), and Na_2CO_3 (1.10 g, 10.4 mmol) in degassed EtOH (3.5 mL), benzene (20 mL) and, H_2O (10 mL) under nitrogen at 80 °C for 96 h followed by column chromatographic purification on silica gel using CH_2Cl_2 as the eluent produced **4e** as a red solid (2.3 g, 72%): mp > 380 °C dec; ^{1}H NMR (400 MHz, $CDCl_3$) δ 10.14 (s, 2H), 8.72 (s, 2H), 8.24 (d, J = 8.4 Hz, 2H), 8.07 (d, J = 8.4 Hz, 4H), 7.85 (t, J = 8.4 Hz, 6H), 7.48 (t, J = 7.6 Hz, 2H), 7.34 (d, J = 7.6 Hz, 4H), 2.73 (septet, J = 6.8 Hz, 4H), 1.20−1.15 (m, 24H); ^{13}C NMR (100 MHz, $CDCl_3$) δ 191.1, 163.0, 162.9, 147.8, 145.4, 139.9, 136.0, 135.2, 134.6, 132.9, 131.4, 130.8, 130.2, 130.1, 129.9, 129.7, 129.3, 128.5, 124.0, 122.6, 122.3, 29.3, 24.2, 24.1; HRFAB *m/z* 919.3757, calcd for *m/z* $C_{62}H_{50}N_2O_6$ 918.3669. Anal. Calcd for $C_{62}H_{50}N_2O_6$: C, 81.02; H, 5.48; N, 3.05. Found: C, 80.80; H, 5.56; N, 2.85.

(19) Hofkens, J.; Vosch, T.; Maus, M.; Kohn, F.; Cotlet, M.; Weil, T.; Herrmann, A.; Müllen, K.; De Schryver, F. C. *Chem. Phys. Lett.* **2001**, *333*, 255−263.
(20) Wipf, P.; Jung, J.-K. *J. Org. Chem*. **2000**, *65*, 6319−6337.
(21) Faraoni, M. B.; Koll, L. C.; Mandolesi, S. D.; Zúòiga, A. E.; Podestá, J. C. *J. Organomet. Chem*. **2000**, *613*, 236−238.
(22) Seaman, W.; Johnson, J. R. *J. Am. Chem. Soc*. **1931**, *53*, 711−723.
(23) Ishida, T.; Mizutani, W.; Choi, N.; Akiba, U.; Fujihira, M.; Tokumoto, H. *J. Phys. Chem. B* **2000**, *104*, 11680−11688.
(24) Park, K. C.; Yoshino, K.; Tomiyasu, H. *Synthesis* **1999**, *12*, 2041−2044.

***N,N′*-Bis(2,6-diisopropylphenyl)-1,7-bis(4-methoxyphenyl)perylene-3,4,9,10-tetracarboxydiimide (4f).** The reaction of **3** (3.0 g, 3.5 mmol), 4-methoxyphenylboronic acid[25] (4.21 g, 27.7 mmol), $Pd(PPh_3)_4$ (100 mg, 2.5 mol %), and Na_2CO_3 (1.10 g, 10.4 mmol) in degassed EtOH (3.5 mL), benzene (20 mL), and H_2O (10 mL) under nitrogen at 80 °C for 8 h followed by column chromatographic purification on silica gel using toluene/CH_2Cl_2 (2:3) as the eluent produced **4f** as a red solid (2.1 g, 66%): mp > 380 °C dec; ^{1}H NMR (400 MHz, $CDCl_3$) δ 8.69 (s, 2H), 8.22 (d, J = 8.0 Hz, 2H), 7.99 (d, J = 8.0 Hz, 2H), 7.54 (d, J = 8.4 Hz, 4H), 7.47 (t, J = 8.0 Hz, 2H), 7.32 (d, J = 8.0 Hz, 4H), 7.02 (d, J = 8.4 Hz, 4H), 3.91(s, 6H), 2.74 (septet, J = 6.8 Hz, 4H), 1.17−1.14 (m, 24H); ^{13}C NMR (100 MHz, $CDCl_3$) δ 163.4, 163.3, 160.0, 145.4, 140.9, 135.8, 135.5, 134.2, 132.8, 130.4, 130.3, 129.8, 129.7, 129.7, 129.5, 128.2, 124.0, 122.1, 121.6, 115.6, 55.5, 29.3, 24.2, 24.1; HRFAB *m/z* 923.4080, calcd for $C_{62}H_{54}N_2O_6$ *m/z* 922.3982. Anal. Calcd for $C_{62}H_{54}N_2O_6$: C, 80.67; H, 5.90; N, 3.03. Found: C, 80.49; H, 5.92; N, 2.99.

***syn*- and *anti*-*N,N′*-Bis(2,6-diisopropylphenyl)-1,7-bis(2,4-dimethoxyphenyl)perylene-3,4,9,10-tetracarboxydiimide (4g).** The reaction of **3** (4.0 g, 4.6 mmol), 2,4-dimethoxyphenylboronic acid[26] (5.04 g, 27.7 mmol), $Pd(PPh_3)_4$ (133 mg, 2.5 mol %), and Na_2CO_3 (1.47 g, 13.5 mmol) in degassed EtOH (4.7 mL), benzene (26.6 mL), and H_2O (13.3 mL) under nitrogen at 80 °C for 16 h followed by column chromatographic purification on silica gel using toluene/CH_2Cl_2 (2:3) as the eluent produced **4g** (two conformational isomers, 1:1 ratio) as a red solid (3.2 g, 70%): mp > 360 °C dec; ^{1}H NMR (400 MHz, $CDCl_3$) δ 8.66 (s, 2H), 8.26 (d, J = 8.0 Hz, 2H), 8.11−8.08 (m, 2H), 7.47 (t, J = 8.0 Hz, 2H), 7.35−7.27 (m, 6H), 6.67−6.62 (m, 4H), 3.92, 3.19 (two s, 6H), 3.70, 3.65 (two s, 6H), 2.78−2.72 (m, 4H), 1.19−1.14 (m, 24H); ^{13}C NMR (100 MHz, $CDCl_3$) δ 163.6, 163.4, 161.5, 156.8, 156.6, 145.5, 145.5, 137.1, 137.0, 136.8, 136.2, 136.1, 134.0, 131.1, 131.0, 130.5, 130.0, 129.4, 128.8, 128.8, 128.2, 128.2, 127.9, 127.7, 123.94, 123.91, 123.7, 121.8, 121.7, 121.6, 106.4, 99.80, 99.75, 55.9, 55.7, 55.6, 29.2, 24.2, 24.13, 24.11, 24.06; HRFAB *m/z* 983.4292, calcd for $C_{64}H_{58}N_2O_8$ *m/z* 982.4193. Anal. Calcd for $C_{64}H_{58}N_2O_8$: C, 78.19; H, 5.95; N, 2.85. Found: C, 77.83; H, 5.97; N, 3.00.

***syn*- and *anti*-*N,N′*-Bis(2,6-diisopropylphenyl)-1,7-bis(2,5-dimethoxyphenyl)perylene-3,4,9,10-tetracarboxydiimide (4h).** The reaction of **3** (3.0 g, 3.5 mmol), 2,5-dimethoxyphenylboronic acid[27] (3.78 g, 20.8 mmol), $Pd(PPh_3)_4$ (100 mg, 2.5 mol %), and Na_2CO_3 (1.10 g, 10.4 mmol) in degassed EtOH (3.5 mL), benzene (20 mL), and H_2O (10 mL) under nitrogen at 80 °C for 16 h followed by column chromatographic purification on silica gel using toluene/CH_2Cl_2 (2:3) as the eluent produced **4h** (two conformational isomers, 1:1 ratio) as a dark red solid (2.5 g, 71%,): mp > 350 °C dec; ^{1}H NMR (400 MHz, $CDCl_3$) δ 8.64 (s, 2H), 8.27 (d, J = 8.4 Hz, 2H), 8.10−8.07 (m, 2H), 7.46 (t, J = 7.6 Hz, 2H), 7.31 (d, J = 7.6 Hz, 4H), 7.01−6.93 (m, 6H), 3.81−3.62 (four s from two different conformational isomers at 3.81 (s, 3H), 3.79 (s, 3H), 3.66 (s, 3H), 3.62 (s, 3H)), 2.78−2.70 (m, 4H), 1.18−1.13 (m, 24H); ^{13}C NMR (100 MHz, $CDCl_3$) δ 163.5, 163.3, 154.7, 154.7, 149.8, 149.6, 145.5, 145.5, 137.00, 136.95, 136.3, 135.8, 135.7, 133.9, 131.92, 131.87, 130.4, 130.3, 129.5, 128.7, 128.6, 128.4, 128.3, 128.2, 123.9, 121.93, 121.87, 116.3, 116.2, 114.4, 114.2, 113.2, 113.1, 56.4, 56.3, 56.0, 55.9, 29.24, 29.21, 24.18, 24.15, 24.1; HRFAB *m/z* 983.4260, calcd for *m/z* $C_{64}H_{58}N_2O_8$ 982.4193. Anal. Calcd for $C_{64}H_{58}N_2O_8$: C, 78.19; H, 5.95; N, 2.85. Found: C, 77.91; H, 6.03; N, 2.64.

***N,N′*-Bis(2,6-diisopropylphenyl)-1,7-bis(4-diphenylamino)phenylperylene-3,4,9,10-tetracarboxydiimide (4i).** The reaction of **3** (3.0 g, 3.5 mmol), 4-(diphenylamino)phenylboronic acid[28] (8.01 g, 27.7 mmol), $Pd(PPh_3)_4$ (100 mg, 2.5 mol %), and Na_2CO_3 (1.10 g, 10.4 mmol) in degassed EtOH (3.5 mL), benzene (20 mL), and H_2O (10 mL) under nitrogen at 80 °C for 72 h followed by column chromatographic purification on silica gel using toluene as the eluent produced **4i** as a dark purple solid (2.47 g, 60%): mp > 400 °C dec; ^{1}H NMR (400 MHz, $CDCl_3$) δ 8.83 (s, 2H), 8.41 (d, J = 8.0 Hz, 2H), 8.23 (d, J = 8.0 Hz, 2H), 7.56−7.52 (m, 6H), 7.42−7.35 (m, 14H), 7.29−7.25 (m, 10H), 7.12 (t, J = 7.6 Hz, 4H), 2.73 (septet, J = 6.8 Hz, 4H), 1.26−1.24 (m, 24H); ^{13}C NMR (100 MHz, $CDCl_3$) δ 162.90, 162.88, 148.1, 146.6, 145.1, 140.6, 135.3, 134.6, 132.4, 130.1, 129.7, 129.5, 129.4, 129.22, 129.19, 129.1, 128.8, 128.0, 124.7, 123.7, 123.6, 123.3, 121.8, 121.4, 29.5, 24.42, 24.37; HRFAB *m/z* 1197.5306, calcd for $C_{84}H_{68}N_4O_4$ *m/z* 1196.5241. Anal. Calcd for $C_{84}H_{68}N_4O_4$: C, 84.25; H, 5.72; N, 4.68. Found: C, 83.90; H, 5.78; N, 4.96.

Acknowledgment. We thank the National Science Council of the ROC, the Ministry of Education, the Ministry of Economy, and the RiTdisplay Corporation for financial support.

Supporting Information Available: ^{1}H and ^{13}C NMR spectra of **3** and **4a**−**4i**, CIF data, the ORTEP diagram for **3**, and the MM2-calculated *XYZ* coordinates for the structures of **4c**−**4f** and **4i**. This material is available free of charge via the Internet at http://pubs.acs.org.

JO050001F

(25) Belloni, M.; Manickam, M.; Wang, Z.-H.; Preece, J. A. *Mol. Cryst. Liq. Cryst*. **2003**, *399*, 93−114.

(26) Schmidt, J. M.; Tremblay, G. B.; Pagé, M.; Mercure, J.; Feher, M.; Dunn-Dufault, R.; Peter, M. G.; Redden, P. R. *J. Med. Chem.* **2003**, *46*, 1289−1292.

(27) He, Z.; Craig, D. C.; Colbran, S. B. *J. Chem. Soc*., *Dalton Trans*. **2002**, 4224−4235.

(28) Pudzich, R.; Salbeck, J. *Synth*. *Met*. **2003**, *138*, 21−31.